

**TECHNICAL PAPER**

Probabilistic corrosion condition assessment of a tunnel structure

Sylvia Keßler^{1,2} ¹Helmut Schmidt University/University of the Federal Armed Forces Hamburg, Hamburg, Germany²Technical University of Munich, Centre for Building Materials, Munich, Germany**Correspondence**Sylvia Keßler, Helmut Schmidt University/ University of the Federal Armed Forces Hamburg, Hamburg, Germany.
Email: sylvia.kessler@hsu-hh.de**Funding information**

Federal Highway Administration of Germany and the Federal Ministry of Transport and Digital Infrastructure, Grant/Award Number: FE 15.0481/2009/DRB; Federal Ministry of Transport and Digital Infrastructure; Federal Highway Administration

Abstract

Reinforced concrete structures constitute the basis of our infrastructure. Their functionality and structural safety is essential to maintain our mobility and the industrial performance of our societies. Unexpected maintenance can lead to serious economic consequences. Most industrial countries are faced with the fact that the reliability of their infrastructure has decreased over the past decades due to ageing and associated durability issues. Most often reinforcement corrosion is the major problem with respect to ageing phenomena observed. Therefore, data from corrosion inspection and their implementation in probabilistic corrosion condition assessment are considered to be of major importance to assist engineers in the maintenance process. Reliable information about the corrosion condition state can be derived through half-cell potential measurements. The half-cell potential measurement method is an easy to apply nondestructive measurement method to detect ongoing corrosion. The procedure on how to update the service life based on a probabilistic treatment of measured half-cell potentials is presented in a case study of a chloride-contaminated reinforced concrete structure. Besides the chosen probabilistic model, major impact on the accuracy of the updated service life has the evaluation of the half-cell potential measurements.

KEYWORDS

condition assessment, half-cell potential measurement, probabilistic approach, reinforcement corrosion, service life prediction

1 | INTRODUCTION

Even though the used materials coped with the specifications of appropriate materials at the time of construction

our infrastructure requires more and more frequent maintenance, repair, or in the worst case partial replacement due to materials degradation. The knowledge on how reinforced concrete interacts with aggressive environment continually improves and consequently specifications are under constant revision. One outcome of the revision process is that an aggressive environment is probably much more aggressive as expected at the time of design especially with regard to exposure to chlorides.¹

Discussion on this paper must be submitted within two months of the print publication. The discussion will then be published in print, along with the authors' closure, if any, approximately nine months after the print publication.

This is an open access article under the terms of the Creative Commons Attribution License, which permits use, distribution and reproduction in any medium, provided the original work is properly cited.

© 2020 The Author. Structural Concrete published by John Wiley & Sons Ltd on behalf of International Federation for Structural Concrete

Furthermore, our infrastructure suffers much higher number of load alternations than they are designed for. The consequence is that with time our ageing infrastructure shows more and more deterioration.²

However, civil engineers need to ensure the structural safety and on the other hand, they need to extend the working life of our existing structures since we cannot replace all deteriorated structures within a short period of time. A reliable condition assessment of each existing concrete structure—with or without visual damage—is the first step in order to achieve these goals. Only the knowledge about the actual structural condition allows a reliable prediction of the future evolution. In this framework, a case study presents the procedure of a reliable corrosion condition assessment of a tunnel structure contaminated over time by external chlorides. Here, the focus is on the evaluation of actual condition with respect to durability during the residual service life.

2 | BACKGROUND

Existing concrete structures exposed to a chloride-laden environment suffer from a high risk with time resulting from corrosion of the reinforcement steel. Especially aged concrete structures are prone to corrosion since durability was a marginal design aspect in former times, which gained much greater significance only in the last few decades. Consequently, existing structures in contact with seawater or de-icing salts from winter maintenance should be subject to regular corrosion condition assessment.

Normally, the high alkalinity of the concrete protects the embedded steel reinforcement against corrosion through the formation of a thin iron oxide layer on the steel surface after the reaction of the hydroxide ions with the iron ions. However, with time chloride ions penetrate through the porous concrete cover and as soon as a critical chloride concentration is achieved at the reinforcement level chloride-induced corrosion becomes likely. In cracked concrete, the transport of chlorides to the reinforcement is even faster and corrosion initiation is unavoidable if no corrosion protection measures are applied. The spot on the reinforcement surface where the chloride threshold level is exceeded first is the spot where the anodic reactions will take place by oxidizing iron and releasing electrons. These electrons reduce water and oxygen into hydroxyl ions at the cathode. Since the concrete pore solution is mostly a very conductive electrolyte, the hydroxide ions will move toward the iron ions and form iron hydroxyl and at a later stage, these will be transformed into iron oxides (rust). A macro-cell element is formed leading to a local loss of cross section at the

anode area. The volume of the resulting corrosion products is several times larger than that of the original steel, which could lead to tensile strains in the concrete matrix. The result is cracking and spalling of the concrete cover that impairs the serviceability and at a later stage the load bearing capacity of a structure. However, the resulting corrosion products may also diffuse into the concrete pore structure without inducing sufficient strain for concrete cracking. Under these circumstances, there is no visual damage at the concrete surface and nondestructive corrosion inspection becomes even more important.

Regarding the corrosion development over time two subsequent stages can be distinguished on concrete structures: the initiation and the propagation stage. The initiation phase is the time period of chloride ingress until a critical threshold level is achieved at the reinforcement. The subsequent propagation phase begins at the moment depassivation of the steel occurs and when the loss of cross section starts. The initiation phase can be described with transport models,^{3,4} whereas the propagation phase is the combination of an electrochemical model based on Faraday's law^{5,6} with fracture mechanics.⁷ The crucial point is that there are no visual signs of corrosion until cracking of the concrete cover. However, when the first corrosion-induced crack formation occurs the propagation phase may be in a well-advanced stage and very costly repair measures are frequently the consequence. Thus, the objective of corrosion condition assessment is to determine whether the structure or the component is still in the initiation phase or already in the propagation phase. In the case of corrosion initiation, the extent of corrosion activity is of interest to plan future repair measures, especially for the reinforcement needed to ensure the load bearing capacity or the serviceability of a structure.

3 | CORROSION INSPECTION

The overall objective of condition assessment is the determination of the residual service life. First, the evaluation of the current corrosion condition is necessary before taking account of time-dependent changes, which may occur. In practice, the most common corrosion inspection method for reinforced concrete structures is the half-cell potential measurement.⁸⁻¹¹ As soon as corrosion is initiated, the anodic area shows much more negative electrochemical potential than the cathodic areas. The potential difference between both areas is the driving potential, which leads to the development of a potential field in the concrete forced by the resulting corrosion current. This potential field is also present on the concrete surface and this fact enables the detection of corrosion of the embedded steel with half-cell potential measurements. An

external reference electrode (e.g. Copper/Copper-Sulfate electrode) is connected to the concrete surface through an electrolytic contact, e.g. a wet sponge, and the potential difference with a voltmeter is measured against the internal reinforcement. The complete concrete surface is scanned by displacement of the reference electrode in a defined grid size. The indication of reinforcement corrosion is the combination of very negative potentials with pronounced potential gradients.¹⁰ The advantage of scanning the half-cell potential is the resulting spatial information about the corrosion condition of a structure.^{12,13} The measurement procedure itself is mostly nondestructive. Only for the electric connection to the reinforcement the concrete needs to be removed at small spots.

However, reinforcement corrosion is an instantaneous process and the half-cell potential measurement can only indicate active corrosion at the time of measurement. Consequently, detection of past or future corrosion activity is impossible. The half-cell potential measurement outcome is of a qualitative nature: either the reinforcement is corroding or not.

3.1 | Reliability of corrosion inspection

According to Matthews et al.¹⁴ testing and monitoring shall assess reliable data on the real condition and behavior of structures, and may enable reduction of uncertainties in the assessment and prediction of the performance of the structures. In order to achieve these objectives the reliability of the corrosion testing system, here the half-cell potential measurement, needs to be known. Generally, the reliability of a qualitative nondestructive inspection method is defined as the degree that the testing system is capable of achieving its purpose concerning detection and false calls. The capability evaluation includes the consideration of the testing procedure, the equipment, and the personnel that performs an NDE inspection.¹⁵ The probability of detection (POD) is the accepted parameter to quantify the inspection reliability. Normally, the POD is described in dependence of the flaw size since the flaw size affects the reliability the most. The same applies to the half-cell potential measurement. Here, the flaw size—the anode area—has a major impact on the detection reliability. With increasing anode area, the corrosion detectability will also increase. On the other hand, heterogeneous moisture conditions and large grid sizes impair the probability of corrosion detection.¹⁶ Figure 1 shows a POD curve of the half-cell potential measurement considering a concrete cover of 50 mm and a grid size of $15 \times 15 \text{ cm}^2$.

The presented POD curve of the half-cell potential measurement copes with the assumptions that with

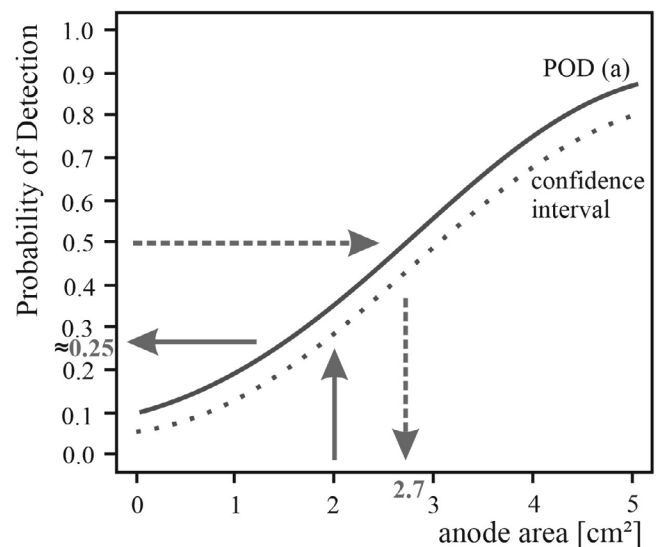


FIGURE 1 Probability of detection curve of the half-cell potential measurement with a concrete cover of 50 mm and a grid size $15 \times 15 \text{ cm}^2$. The dotted line indicates the 95% confidence interval

increasing defect size the detectability also increases. A defect size of 2.7 cm^2 will be detected with a probability of 50% if a high concrete cover is present and a grid size of $15 \times 15 \text{ cm}^2$ is chosen. The advantage of the POD curve is that as soon as a critical defect size a_{crit} is known, the corresponding probability level of detectability can be read off. If we assume a critical effect, size of 2 cm^2 the $\text{POD}(a_{\text{crit}}) \approx 0.25$. The POD provides useful information on the capability of the inspection method but it also delivers useful information for updating the working life based on the Bayesian approach.¹⁷

3.2 | Working life prediction

The determination of the remaining service life on a probabilistic basis requires first the estimation of the a-priori depassivation probability. The fib Model Code for Service Life Design³ presents a model to allow for this taking into account the concrete resistance against chloride ingress with regard to the severity of the chloride exposure. Here, the limit state function (Equation 1) describes the time when the critical chloride concentration reaches the depth of the reinforcement:

$$g(X, t) = C_{\text{crit}} - C(c, t_{\text{SL}}) \quad (1)$$

with: C_{crit} , critical corrosion-inducing chloride concentration (wt%/b); $C(c, t)$, chloride concentration at reinforcement depth at time t (wt%/b); c , concrete cover (mm).

The transport model for chloride ingress itself is presented in Equation (2):

$$C(x,t) = C_0 + (C_{S,\Delta x} - C_0) \cdot \left[1 - \operatorname{erf} \frac{x - \Delta x}{2 \cdot \sqrt{D_{\text{app}}(t) \cdot t}} \right] \quad (2)$$

with: $C(x,t)$, depth- and time-dependent chloride concentration (wt%/b); C_0 , initial chloride concentration (wt%/b); $C_{S,\Delta x}$, chloride concentration at depth Δx (wt%/b); Δx , depth of the convection zone (m); x , depth with a corresponding concentration of chlorides (m); t , time (s); $D_{\text{app}}(t)$, apparent chloride diffusion coefficient (m^2/s).

It should be pointed out that the presented model³ describes only the chloride ingress in uncracked concrete.

After corrosion inspection, the a-priori depassivation probability can be updated following the Bayesian approach, which describes how the conditional probability of an event A given the occurrence of another event E can be computed from the unconditional $P(A)$ and from $P(E|A)$ (Equation 3):

$$P(A|E) = \frac{P(A \cap E)}{P(E)} = \frac{1}{P(E)} P(E|A) P(A) \quad (3)$$

In the context of this paper, the event A represents the event of reinforcement corrosion (C), whereas the event E is the indication of reinforcement corrosion (I). The specific topic of updating the corrosion probability can be expressed in the following way (Equations 4 and 5)¹⁷:

$$P(C|I) = \frac{P(I|C) \cdot P(C)}{P(I|C) \cdot P(C) + P(I|\bar{C}) \cdot P(\bar{C})} \quad (4)$$

$$P(\bar{C}|\bar{I}) = \frac{P(\bar{I}|\bar{C}) \cdot P(\bar{C})}{P(\bar{I}|\bar{C}) \cdot P(\bar{C}) + P(\bar{I}|C) \cdot P(C)} \quad (5)$$

with: C , corrosion; I , indication.

$P(C|I)$ is the probability of corrosion given that the reinforcement is corroding in dependence that the indication of reinforcement corrosion is positive. In contrast, $P(\bar{C}|\bar{I})$ is the probability of the reinforcement being passive given that no corrosion is indicated. Both conditional probabilities provide important information for the subsequent decision-making process whether the structure needs to be repaired or to plan the next corrosion inspection.

3.3 | Case study: Tunnel structure

The case study is a tunnel structure in the south of Bavaria built in 1995. According to the documentation, a

Portland cement was used for the concrete composition that is referred to as complying with a strength class B25. No information about the water-to-binder ratio has been available and therefore a value of 0.5 is assumed. The nominal concrete cover from the documentation is extreme with a value of 60 mm. Due to the winter road maintenance with application of de-icing salts the inner wall surfaces of the tunnel structure are exposed to chloride-contaminated splash and spray water during the winter period. All yearlong drying and wetting cycles can be expected due to splash and spray water from the cars and trucks depending on the rain intensity.

3.4 | General inspection results

The inspection of the tunnel structure was executed in 2014 after being approximately 18 years in service. The inspection routine included a visual inspection, the determination of the concrete cover depth, the sampling of chloride profiles and the measurement of the half-cell potentials. The tunnel is nearly 400 m long and the visual inspection showed cracks and occasional exposed reinforcement and honeycombs. The probing of selected spots based on the half-cell potential measurement results also revealed some spots with loss of reinforcement cross section.

The results of the concrete cover depth measurement showed a mean value of about 60 mm with a SD of about 6 mm (see Table 1). Thus, the real cover depth is in good agreement with the concrete cover design data of the structure. In total 12 chloride profiles were taken at different locations along the length of the tunnel as well as on different heights of the tunnel in uncracked areas. Each chloride profile consists of 6–7 layers with a thickness of 10 mm each. Therefore, sufficient data were available to fit the surface chloride concentration and the apparent chloride diffusion coefficient for each profile. The chloride concentration of the first layer (0–10 mm) is not considered for the fitting to exclude the influence of the convection zone. Figure 2 shows the results of the apparent chloride diffusion coefficient D_{app} and the surface chloride concentration C_s determined from samples taken from different heights of the tunnel structure.

The apparent chloride diffusion coefficient is characterized by a mean value of $0.95 \times 10^{-12} \text{ m}^2/\text{s}$ ($SD \sigma = 0.45 \times 10^{-12} \text{ m}^2/\text{s}$) which is in a range that could be expected for a Portland cement concrete at an age of 20 years. There is no notable dependency of the apparent chloride diffusion coefficient with regard to the height of the tunnel structure. The surface chloride concentration characterized by a mean value of 3.25 wt%/b (SD

TABLE 1 Model input parameters for the α -priori depassivation probability calculation

Parameter	Unit	Distribution	μ	σ	Source
D_{app}	$10^{-12} \text{ m}^2/\text{s}$	Normal	0.95	0.45	Measured
α_{RCM}	—	Beta	0.30	0.12	^{3,4}
t_0	a	Constant	18		Documentation
t	a	Constant	100		
T_{ref}	K	Constant	293		^{3,4}
T_{real}	K	Normal	283	7	Nearest weather station
b_e	K	Normal	4800	700	^{3,4}
$C_{S,\Delta x}$	wt%/b	LogNormal	3.25	1.23	Measured
Δx	mm	Beta (0; 50)	10	5	^{3,4}
C_{crit}	wt%/b	Beta (0.2; 2.0)	0.6	0.15	^{3,4}
C_0	wt%/b	Constant	0		Assumed
c	mm	Normal	60	6	Measured

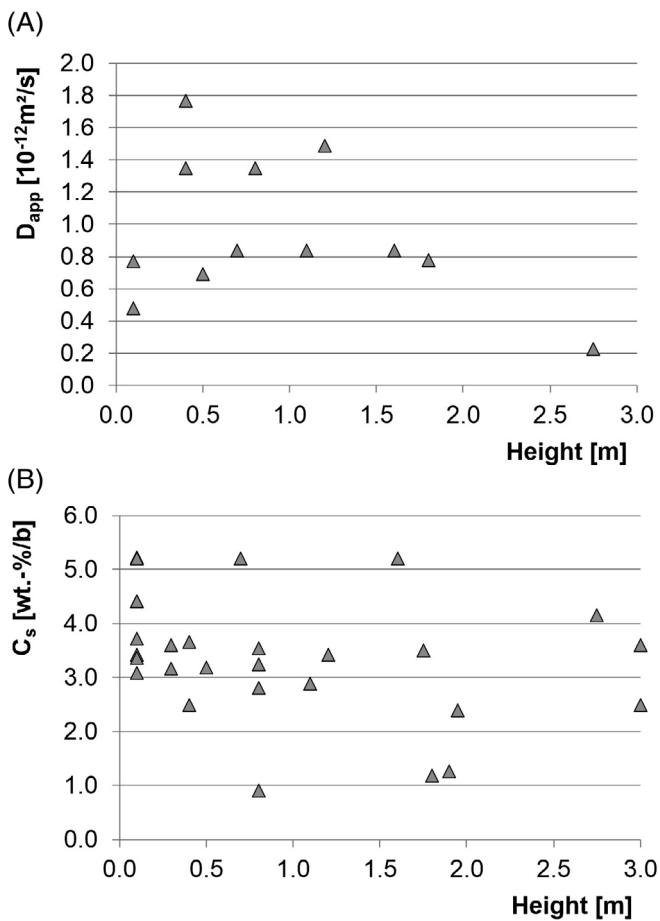


FIGURE 2 The results of the apparent chloride diffusion coefficient D_{app} and the surface chloride concentration C_s as function of the height of the tunnel structure

$\sigma = 1.23$ wt%/b) is high. Some chloride profiles show surface chloride concentrations of over 5.0 wt%/b. This value is much higher than normally assumed for infrastructure

under de-icing salt exposure with wet and dry cycles.⁴ Thus, the structure shows high chloride contamination independent of the location in the tunnel structure. Due to its microclimate and traffic movements, the chloride-contaminated water is intensively subjected to turbulence leading to a distribution of the chlorides over the whole structure. Additionally, there is no clear dependency of the apparent chloride diffusion coefficient D_{app} and the surface chloride concentration C_s with regard to the tunnel length (data not presented here).

3.5 | A-priori depassivation probability

Now, all data are available to calculate the a-priori depassivation probability according to fib Model Code for Service Life Design.³ Table 1 shows the overview of all input parameters.

The data of three input parameters (D_{app} , $C_{S,\Delta x}$, c) result from the inspection of the structure. For the determination and validation of their distribution function Kolmogorov-Smirnov tests are performed. However, it should be noted that the data set of the apparent chloride diffusion coefficient and the surface chloride concentration is very small.

Figure 3 presents the a-priori depassivation probability of the tunnel structure with time. The approximation of the limit state function, Equation (1), is performed according to the second order reliability method.

After approximately 20 years in service the tunnel structure has a depassivation probability of 13% which corresponds to a reliability index of $\beta = 1.1$ assuming that the depassivation probability follows normal distribution. The prediction of the corrosion probability reveals that the corrosion probability increases up to 37% (reliability

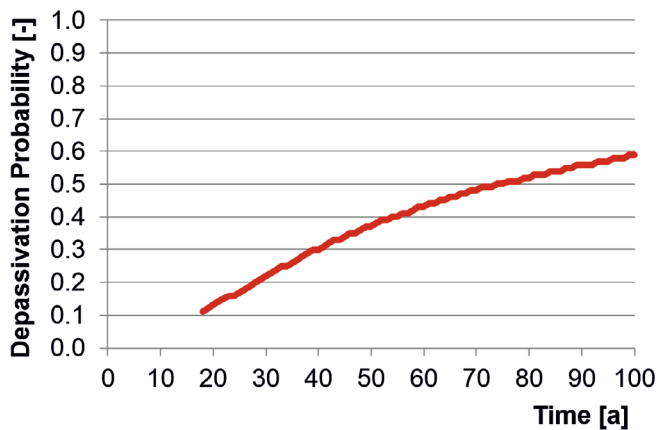


FIGURE 3 A-posteriori depassivation probability of the tunnel structure with time

index $\beta = 0.33$) until the age of 50 years. Even though the concrete cover depth is much higher than required by codes and even with the found low apparent chloride diffusion coefficient the structure is vulnerable to chloride-induced corrosion due to the very high chloride surface concentration.

The calculated depassivation probability provides useful information about the expected current corrosion behavior of the concrete structure. Nevertheless, for further evaluation and condition assessment spatial information about the corrosion condition state is necessary. Even though the structure does not show spatial dependency of the measured surface chloride concentration, the spatial variability of the deterioration process could also be the result of exposure-related local peculiarities, e.g. gradient condition, puddle formation locally at the foot of the wall, etc., and/or material inhomogeneity. Taken into account the calculated relatively high corrosion probability half-cell potential measurements are performed to enable the comparison of the real corrosion condition state with the calculated corrosion probability and to provide spatial information about the corrosion condition.

3.6 | Inspection data with spatial information

The half-cell potential measurements were executed according to the Specification B3¹⁰ with a grid size of $13 \times 13 \text{ cm}^2$. This grid size is much smaller than normally used but the concrete surface had a uniform linear texture due to the formwork that enabled an easy orientation during measurement. For the sake of simplicity, the following study focuses on one single tunnel segment with a size of 10 m length and 3 m height. The visual

inspection revealed stress-induced cracks as shown later in Figure 7. The results of concrete cover depth measurement (grid size $25 \times 50 \text{ cm}^2$) are mapped next to the half-cell potential measurement data, see Figure 4, as to consider all spatial information. The spot without any data is the position of a mounting system.

The concrete cover depth is more or less equally distributed over the whole segment. Higher cover depth are found at the bottom of the right side while lower cover depths are in the upper corner on the left side. However, the cover depths are relatively large with values ranging from 35 mm until 70 mm. The half-cell potentials show a different pattern. With increasing height, the potential values become less negative, which is a typical potential distribution in vertical elements. The higher the position on the tunnel wall the less negative is the measured half-cell potential due to higher concrete resistivity.¹⁸ The negative potentials with a pronounced potential gradient are at the bottom especially in between 1 and 2 m longitude. Here, a high probability of reinforcement corrosion is expected. The half-cell potential data provide no information on the crack distribution. Either the crack-crossing reinforcement is not corroding during the time of measurement or the resistance in the crack region is too high to enable proper corrosion detection.

Before applying the Bayesian approach, Equations (3–5), the half-cell potential data need to be analyzed statistically. For this purpose, distinction is necessary whether the reinforcement is active or passive. The aim is to find two normal distribution representing active and passive reinforcement out of the entire half-cell potential data. Figure 5 shows the histogram of the measured half-cell potentials and the corresponding best-fit probability density function for the actively corroding and passive reinforcement, respectively.

The population of the half-cell potentials is in a range of -450 to $-150 \text{ mV}_{\text{CSE}}$. The probability density functions of the active and passive potentials intersect approximately at $-350 \text{ mV}_{\text{CSE}}$. Half-cell potentials in the range of -400 to $-300 \text{ mV}_{\text{CSE}}$ could belong either to the active or to the passive probability density function. Half-cell potentials less negative than $-300 \text{ mV}_{\text{CSE}}$ belong to the passive reinforcement. However, a threshold potential has to be defined in order to enable a clear differentiation if a measured potential indicates an active or a passive corrosion condition state. This threshold value needs to be defined carefully since a too positive threshold bears the risk that corroding areas are overlooked. On the other hand, a too negative threshold leads in the worst case to unnecessary maintenance and repair. Here, the threshold potential is chosen to be the 80% quantile¹⁹ of the active probability density function

FIGURE 4 The half-cell measurement (potential vs. Copper/Copper-sulphate electrode) and the concrete cover depth of the selected segment of the tunnel structure

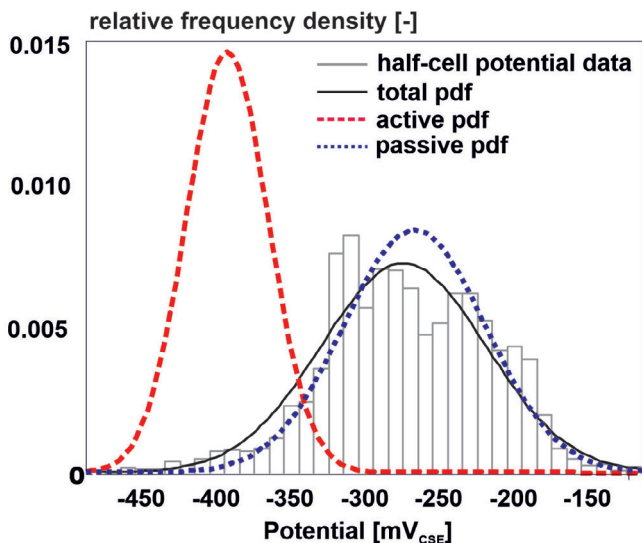
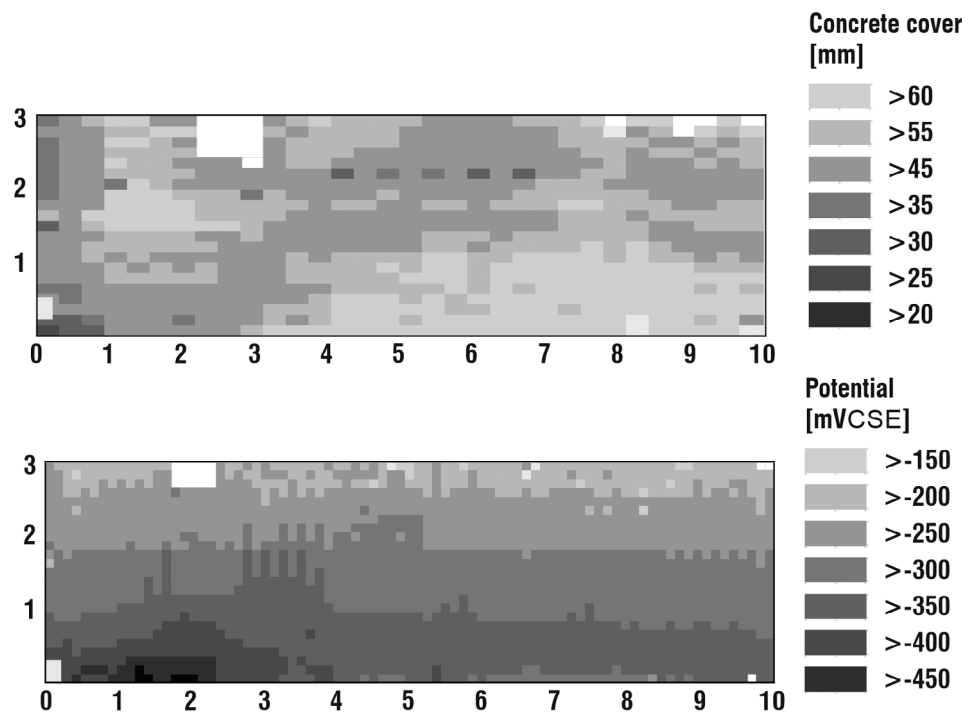


FIGURE 5 Histogram of the half-cell potentials and the corresponding probability density function for the active and the passive reinforcement

with a value of $-365 \text{ mV}_{\text{CSE}}$. This results in the following probabilities:

$$P(I|C) = 0.80 \quad P(\bar{I}|C) = 0.20$$

$$P(\bar{I}|\bar{C}) = 0.82 \quad P(I|\bar{C}) = 0.18$$

Now, all data are available to perform the update of the depassivation probability with the half-cell potential

data based on the Bayesian approach, see Equations (4) and (5).

3.7 | Depassivation probability

Now, the focus is to use the information coming from the half-cell potential scan for the update of the service life prediction. To maintain the spatial corrosion information the segment is divided into elements. The element size ($13 \times 13 \text{ cm}^2$) corresponds to the grid size used for the half-cell potential measurements. Each element is updated with the Bayesian approach individually neglecting the spatial dependency among the elements according to the following steps:

- 1 First, the depassivation probability of each element is recalculated with the associated measured cover depth using Equations (1) and (2). So, the spatial information from the cover depth scan is maintained, see Figure 6.
- 2 Second, the Bayesian updating is performed for each element using Equations (4) and (5), see Figure 6.

The transition of the half-cell potentials to a depassivation probability shows very clearly where the tunnel segment is subjected to a high corrosion probability and where not. One spot with high corrosion probabilities over 85% is at the bottom of the left side from 1 to 3 m length and up to 0.8 m height. In comparison to this

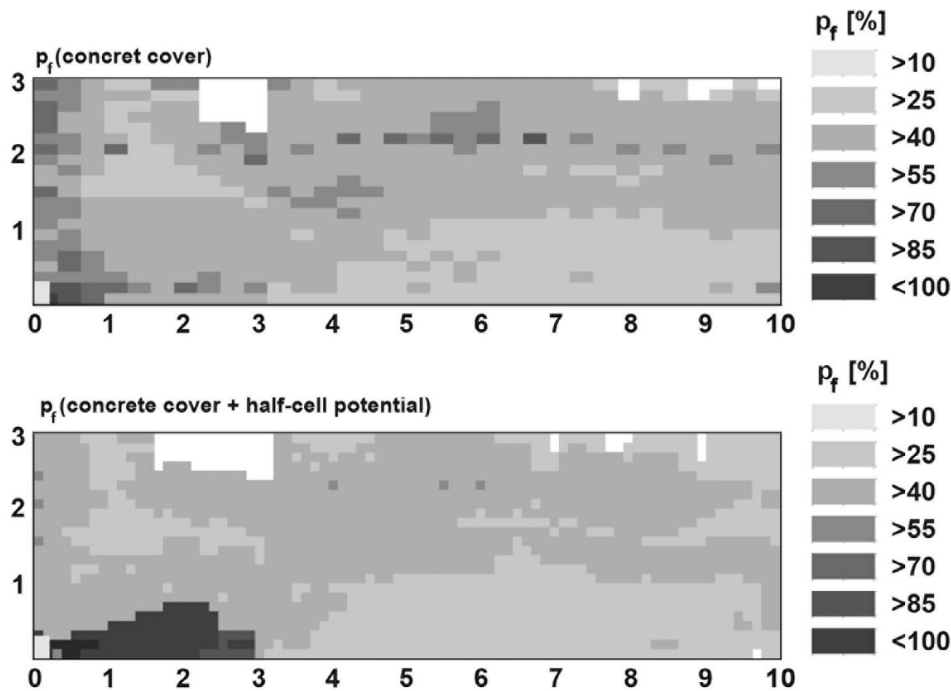


FIGURE 6 Corrosion probability after updating with concrete cover depths and half-cell potentials

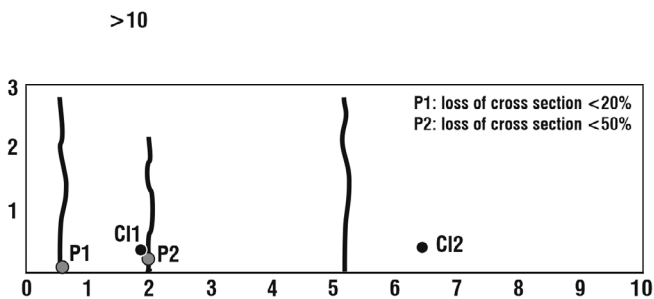


FIGURE 7 Results of the visual inspection and the reinforcement probing

spot, the rest of the tunnel segment seems to be in passive corrosion condition.

According to Figure 3, the calculated overall corrosion probability of the tunnel is about 13%, which fits very well with the spatial corrosion probability of Figure 6. This information gives a very important first orientation about corrosion condition and can serve as an indicator if further corrosion inspection is needed. However, the chloride ingress model of the Model Code for Service Life Design³ considers a smeared chloride exposure with a high *SD* within the structure. For a tunnel structure, especially for vertical components, this is often not the case since the splash water reaches only a certain height of the tunnel wall. In this area, the concrete surface will be exposed to more wet/dry cycles and faster chloride ingress is normally the consequence. Thus, with increasing structure age the half-cell potential

measurement displays indirectly the spatial distribution of the chloride distribution. Consequently, the half-cell potential measurement provides very useful information about corrosion condition of a structure.

Finally, the corrosion condition evaluation is compared to the results from the visual inspection and reinforcement probing, see Figure 7.

The visual inspection reveals three vertical cracks, which show a typical pattern of cracks due to restraint stresses. Fast chloride ingress can be expected in the cracked areas. Two chloride profiles—one in the cracked area (Cl1) and one in an uncracked part (Cl2)—confirm the expectation. The chloride concentration at the reinforcement level in the cracked area is higher than 4.0 wt%/b and in the uncracked area only less than 1.0 wt%/b. The reinforcement is visually examined at two spots, P1 and P2, where the tunnel segment demonstrates high corrosion probabilities. At both spots, loss of cross section was found with up to 50% loss of steel cross sectional area. Both results of the chloride concentration and the visual examination of the reinforcement confirm the results of the probabilistic corrosion condition assessment.

4 | DISCUSSION

The case study presents a procedure to update the corrosion probability based on half-cell potential measurements

with the Bayesian approach. The advantages of the procedure are that half-cell potential results are transferred to condition reliability/corrosion probability that enables a probabilistic condition assessment. Additionally, this procedure maintains the spatial information about the deterioration condition. This information is essential to determine the position of future inspection or in an advanced deterioration stage to estimate the extent of repair measures. This procedure is applicable to assess the corrosion condition of any type of chloride-contaminated structures.

However, the reliability of the corrosion condition assessments depends besides the depassivation probability mainly on the reliability of the measurement method itself, in this case the half-cell potential measurement. The reliability of corrosion detection with half-cell potential measurement depends on several factors such as the chosen inhomogeneous moisture condition,^{16,18} grid size,^{18,20} stochastic evaluation method,²¹ and the chosen threshold potential, the quantile of the anodic probability density function.¹⁹

In the case of inhomogeneous moisture conditions, the corrosion detectability decreases dramatically in comparison to half-cell potential measurements under uniform moisture condition.^{16,21} Due to changing environmental condition, the concrete resistivity varies spatially and temporally, e.g. a structure is exposed to different conditions such as sheltered and unsheltered from rain or located within the tidal range. The consequence is that the clear separation of the half-cell potentials into anodic and cathodic probability density function is compromised since the half-cell potential measure for surface areas exposed to similar moisture conditions form own populations. Therefore, areas with different moisture conditions should be evaluated separately.

The dependency between grid size and corrosion detectability is logical, the smaller the grid size as higher is the reliability of corrosion detection.^{16,20} However, this factor is under the responsibility of the corrosion surveyor and is therefore easy to keep under control. Depending on the needed reliability of corrosion detection, the grid size should be in the range of $10 \times 10 \text{ cm}^2$ up to $20 \times 20 \text{ cm}^2$. In the case of high requirements on the probability of corrosion detection a grid size of $10 \times 10 \text{ cm}^2$, whereas for ordinary corrosion inspections a grid size of $15 \times 15 \text{ cm}^2$ is suitable. This statement is in line with the grid size recommendations of the common guidelines.^{9,10} Larger grid sizes than $20 \times 20 \text{ cm}^2$ lead to poor corrosion detectability.

The half-cell potential evaluation method has a significant impact on the reliability of corrosion inspection.²¹ Although one standard⁸ mentions the evaluation concerning an absolute potential threshold value, the corresponding corrosion detectability is very poor and

consequently such an evaluation method is considered very unreliable. Other applicable statistical evaluation methods are the evaluation of the half-cell potentials based on cumulative distribution function and the probability density function.^{9,11,22} The direct comparison of both evaluation methods shows higher reliabilities in favor of the evaluation method according to the probability density functions.²¹ Here, after the separation of the anodic and cathodic probability density function the threshold potential has to be defined to enable the distinction between corroding and noncorroding areas. The selection of the threshold potential a quantile of the anodic probability density function can affect the reliability of corrosion detection dramatically.¹⁹ The higher the threshold potential the higher is the corrosion detectability, but it increases also the Probability of False Alarm. Both parameters, the POD and the Probability of False Alarm should be in reasonable relation considering the requirements of the corrosion inspection, which needs to be defined for each structure and each inspection individually. Thus, a recommendation of fixed quantile as a threshold potential is not feasible. Each set of half-cell potential measurements results in one probability density function for the active and one function for the passive potentials. Therefore, the threshold potential has to be determined on the one hand considering the probability density functions and on the other hand on taking into account the acceptable degree of Probability of False Alarm.¹⁹ This procedure implies that the surveyor in charge of the evaluation should be an expert on reinforcement corrosion and should directly communicate with the responsible structural engineer. The structural engineer shall evaluate the critical hot spots of the structures under investigation to enable the determination of the acceptable degree of Probability of False Alarm.

All the abovementioned factors should be considered before performing the corrosion condition assessment procedure presented in this case study and even before performing the half-cell potential measurements on the structure. Nevertheless, additional inspection methods such as concrete cover depth measurements, chloride profiles, probing, or concrete resistivity measurement should support the corrosion condition assessment.

5 | CONCLUSIONS

The following conclusions can be drawn from the present study:

- 1 The data from half-cell potential measurements enable the update of the service live prediction.

- 2 The information about spatial variability of chloride-induced reinforcement corrosion on a structure is maintained. After the division of the structure into elements according to the grid size, each element can be assigned to a reliability index or corrosion probability, respectively.
- 3 Major factors influencing the reliability of the updated corrosion probability are:
 - a Anode area (defect size)
 - b (Chosen) grid size
 - c Evaluation method—determination of the threshold potential
 - d (Heterogeneous) moisture condition—concrete resistivity
- 4 The half-cell potential grid size should be adapted according to the needed measurement reliability in order to cope with the requirements from the structural engineer including the probability that in critical regions the steel cross sectional area is reduced to such an extent that the structural safety of the structure is endangered.
- 5 The planning of future inspection or the dimensioning of further repair measures can be performed more economically.

ACKNOWLEDGEMENTS

The author wishes to thank the engineering consultancy Ingenieurbüro Schießl Gehlen Sodeikat GmbH and the Highway Authority of Southern Bavaria for supporting the project by providing the measurement data. The results are part of the research project FE 15.0481/2009/DRB funded by the Federal Highway Administration of Germany and the Federal Ministry of Transport and Digital Infrastructure.

ORCID

Sylvia Kefßler  <https://orcid.org/0000-0002-1335-1104>

REFERENCES

1. Schießl-Pecka A, Willberg U, Rausch A, Bäumler W. 100 years durability for bridge and tunnel constructions—The variable 3-stage concept (100 Jahre Dauerhaftigkeit für Brücken- und Tunnelbauwerke). *Beton- und Stahlbetonbau*. 2018), Heft 10; 113:746–755. <https://doi.org/10.1002/best.201800032>.
2. BAST: Brücken an Bundesfernstraßen, Brückenstatistik 09/2018. Available from www.bast.de
3. fib bulletin 34: Model code for service life design, International Federation for Structural Concrete, Lausanne, Switzerland, ISBN 978-2-88394-074-1 (2006). <https://doi.org/10.35789/fib.BULL.0034>.
4. fib bulletin 76: Benchmarking of deemed-to-satisfy provisions in standards—Durability of reinforced concrete structures exposed to chlorides, International Federation for Structural Concrete, Lausanne, Switzerland, ISBN 978-2-88394-116-8 (2015)
5. Beck M, Burkert A, Harnisch J, et al. Deterioration model and input parameters for reinforcement corrosion. *Struct Concrete*. 2013;13(3):145–155. <https://doi.org/10.1002/suco.201200004>.
6. Otieno MB, Beushausen H, Alexander M. Modelling corrosion propagation in reinforced concrete structures—A critical review. *Cement Concrete Compos*. 2011;33(2):240–245. <https://doi.org/10.1016/j.cemconcomp.2010.11.002>.
7. Bohner, E.. Rissbildung in Beton infolge Bewehrungskorrosion, Dissertation KITopen-ID: 1000041761, Karlsruhe 2013
8. ASTM C876-09 (2009). Standard test method for corrosion potentials of uncoated reinforcing steel in concrete. West Conshohocken, PA: ASTM International.
9. Elsener B, Andrade C, Gulikers J, Raupach M. Half-cell potential measurements—potential map-ping on reinforced concrete structures. *RILEM TC 154-EMC. Mater Struct*. 2003;36(261):461–470. <https://doi.org/10.1007/BF02481526>.
10. DGZfP Specification B3 (2014). Electrochemical half-cell potential measurements for the detection of reinforcement corrosion. German Society for non-destructive Testing
11. SIA Merkblatt 2006 (2013). Planung, Durchführung und Interpretation der Potentialfeldmessung an Stahlbetonbauten. Schweizerischer Ingenieur- und Architekten-Verein (in German)
12. Kefßler, S.; Huber, M.; Straub, D.; Gehlen, C.; Moormann, C.. Stochastic evaluation of active corroding areas in concrete structures. In: 8th International Probabilistic Workshop, 2010, Szczecin, Poland.
13. S. Kefßler, M. Huber, D. Straub, C. Gehlen. Spatial variability of potential fields in reinforced concrete structures. *ICASP* (2011), Zurich.
14. Matthews S, Bigaj-van Vliet A, Walraven J, Mancini G, Dieteren G. fib Model Code 2020: Towards a general code for both new and existing concrete structures. *Struct Concrete*. 2018;19(4):969–979. <https://doi.org/10.1002/suco.201700198>.
15. Müller C, Rosenthal M, Gaal M, Guelle D, Lewis A, Sieber A. Performance demonstration for humanitarian demining. *MP Materialprüfung*. 2003;45(11–12):504–512. Carl Hanser Verlag, München.
16. Kessler S, Gehlen C. Reliability evaluation of half-cell potential measurement using POD. *J Infrastruct Syst*. 2017;23(2). [https://doi.org/10.1061/\(ASCE\)IS.1943-555X.0000334](https://doi.org/10.1061/(ASCE)IS.1943-555X.0000334).
17. Kessler, S.; Gehlen, C.. Probability of detection of potential mapping and its impact on service life prediction. In: Proceeding 12th international conference on applications of statistics and probability in civil engineering, ICASP12 Vancouver, Canada, July 12-15, 2015. Available from: <http://hdl.handle.net/2429/53300>.
18. Kefßler S, Gehlen C. Studie zur Potentialfeldmessung an 40 Jahre alten Stahlbetonbauteilen vom Olympiastadion München—Einfluss des Elektrolytwiderstands und des Messrasters.

- Beton- und Stahlbetonbau. 2013), Heft 9;108:620–629. <https://doi.org/10.1002/best.201300037>.
19. Keßler, S. Evaluation of half-cell potential measurement and its impact on the condition assessment. In: Caspeele, Taerwe & Frangopol, editors. Proceeding IALCCE 2018 life-cycle analysis and assessment in civil engineering: Towards an integrated vision. London: Taylor & Francis Group; 2019. ISBN 978-1-138-62633-1.
 20. Keßler, S.. The reliability of corrosion detection with regard to chosen grid size. In: RILEM Spring Convention and Sustainable Materials, Systems and Structures Conference, Rovinj, Croatia, 18–22 2019
 21. Keßler, S.; Gehlen, C. Reliability of corrosion detection in reinforced concrete structures—impact of the half-cell potential evaluation. In: Bakker, Frangopol & van Breugel, editors. Proceeding IALCCE 2016, life-cycle and sustainability of civil infrastructure systems. London: Taylor & Francis Group, 2016. ISBN 978-1-138-02847-0.
 22. Lentz A. Potentialmessungen zur Unterhaltungsplanung bei Stahlbetonbauten. Institut für Baustatik und Konstruktion, ETH Zürich: Diplomarbeit, 2001.

AUTHOR BIOGRAPHY



Sylvia Keßler
Helmut Schmidt University/ University of the Federal Armed Forces
Hamburg
Hamburg, Germany.
Email: sylvia.kessler@hsu-hh.de

How to cite this article: Keßler S. Probabilistic corrosion condition assessment of a tunnel structure. *Structural Concrete*. 2020;1–11. <https://doi.org/10.1002/suco.201900414>